Journal of Catalysis **191,** 430–437 (2000)
doi:10.1006/jcat.1999.2787, available online at http://www.idealibrary.com on IDEAL®

Influence of the Preparation of Au/Al_2O_3 on CH_4 Oxidation Activity

R. J. H. Grisel,* P. J. Kooyman,† and B. E. Nieuwenhuys*,[1]

*Leiden Institute of Chemistry, Department of Heterogeneous Catalysis and Surface Chemistry, Gorlaeus Laboratoria, P.O. Box 9502, 2300 RA Leiden, The Netherlands; and †National Centre for High Resolution Electron Microscopy, Delft University of Technology, Rotterdamseweg 137, 2628 AL Delft, The Netherlands

Received September 29, 1999; revised November 29, 1999; accepted December 22, 1999

Four different Au/Al_2O_3 catalysts were prepared via impregnation and deposition precipitation. The preparation technique used was found to have a large influence on the average Au particle size and amounts of Au adsorbed. For CH_4 oxidation a clear particle size effect was observed, in which small Au particles are beneficial for high activity. From the preparation methods studied, homogeneous deposition precipitation leads to the smallest average particle size (3–5 nm) and, hence, to the most active catalysts. These catalysts, however, showed some sintering of Au accompanied by a slight deactivation during catalytic reaction. The results do not support the idea of ionic Au being responsible for the catalytic activity.

Key Words: **CH_4; oxidation; gold; Al_2O_3; particle size effect; preparation.**

1. INTRODUCTION

Bulk gold is generally regarded to be catalytically inactive. However, recently very small, well-dispersed Au particles have been found to have high catalytic activity for various reactions. These reactions include the hydrogenation of CO and CO_2 (1–3), hydrochlorination of acetylene (4, 5), and reduction of NO (6–11). The most surprising results, however, have been achieved in low temperature CO oxidation (12–22). For example, Au/TiO_2 (17–21) and Au/Fe_2O_3 (19–22) are already capable of CO oxidation at room temperature.

The high activity of supported Au catalysts in CO oxidation mainly depends on the Au particle size and the presence of suitable metal oxides (MO_x). The nature of the active species is still under discussion. It has been suggested that the activity of Au/MO_x catalysts can be attributed to the presence of small Au particles, which are stabilized by the MO_x (19, 21, 23). The high activity has been ascribed to the presence of ionic Au species (23) or metallic Au (19, 21, 24). It has also been proposed that the reaction solely takes place at the Au/MO_x interface, with CO adsorbed on Au and MO_x the supplier of O (25).

[1] Fax: +31 71 527 44 51. E-mail: nieuwe_b@chem.LeidenUniv.nl.

The high activity observed for CO oxidation over Au-based catalysts instigated studies concerning several other oxidation reactions such as the oxidative destruction of dichloromethane (26), the epoxidation of alkenes (27–29), and the complete oxidation of CH_4 (30, 31).

Waters *et al.* (30) reported that coprecipitated Au on several transition metal oxides was remarkably active in the total oxidation of CH_4. For example, coprecipitated Au/Co_3O_4 was reported to have a light-off temperature just lower than 250°C. In comparison, fresh Pd/Al_2O_3 is only active at temperatures around and above 300°C (32, 39, 40). However, under reaction conditions Pd/Al_2O_3 catalysts typically become more active with time on stream (39). The low temperature activity observed for Au supported on transition metal oxides was accredited to the presence of Au in an oxidized state (30). Au/MgO catalysts were also found to be active in CH_4 oxidation (31). Addition of already small amounts of Au (0.04 wt%) was found to inhibit the production of methane-coupling products, which are characteristic of bare MgO. Instead, the yield of CO was found to increase with low Au loadings (<2 wt%), whereas a higher Au loading induced high selectivity to CO_2.

In spite of the great interest in the particle size effect in low temperature CO oxidation, no systematic study has been performed yet concerning the effect of the Au particle size on the activity in CH_4 oxidation reactions. In addition, little is known about the stability of these catalysts at the relatively high temperatures needed for CH_4 oxidation. The present paper deals with the influence of the preparation method on the Au particle size, and the catalytic activity for the complete oxidation of CH_4.

2. EXPERIMENTAL

2.1. Catalyst Preparation

In this study γ-Al_2O_3 (Engelhard, code: Al-4172 P) was chosen as support, because of its high surface area, thermal stability, and relative inertness toward steam, which is one of the reaction products. The specific surface area was determined to be 200 $m^2\ g^{-1}$ and the pore volume was

0021-9517/00 $35.00

about 2.8 ml g^{-1}. $HAuCl_4$ (Aldrich, 99.999%) was used as precursor. The intended Au loading was 5 wt% on all samples. The Au/Al_2O_3 catalysts were prepared via pore volume impregnation, wet impregnation, and homogeneous deposition precipitation (HDP) with either Na_2CO_3 (Merck, p.a.) or $NH_2(CO)NH_2$ (Acros, p.a.) as precipitating agent.

To remove water and air out of the pores of the support, Al_2O_3 was dried in air at 80°C for at least 16 h and subsequently evacuated for 1 h while cooling to room temperature. Under vacuum a certain volume of an aqueous $HAuCl_4$ solution, corresponding to the pore volume of the used amount of support, was added with an injection syringe. After the solution had been taken up in the pores of the support, air was admitted into the flask and the sample was kept at room temperature until the external edges had dried *(catalyst A)*.

An aqueous solution of $HAuCl_4$ was added to Al_2O_3. The suspension was vigorously stirred and kept at 70°C until the solvent had evaporated *(catalyst B)*.

An aqueous solution of $HAuCl_4$ was added to Al_2O_3 and kept at 70°C. Under vigorous stirring, a diluted solution of Na_2CO_3 in demineralized water was added dropwise to increase the pH of the solution. When the pH of the solution was 8, the slurry was filtered, washed, and dried at ambient conditions until the external edges had dried *(catalyst C)*.

An aqueous solution of $HAuCl_4$ and excess $NH_2(CO)NH_2$ were added to Al_2O_3. The suspension was vigorously stirred and kept at 70°C until the pH reached 8. The slurry was filtered, washed, and dried at ambient conditions *(catalyst D)*.

Finally, all samples were further dried in air at 80°C for at least 16 h and reduced in a flow of pure H_2 up to 300°C (heating rate 5°C min^{-1}). The samples were kept at 300°C for 30 min and then cooled to room temperature under a flow of H_2. Air was admitted cautiously, and the samples were stored under normal atmosphere at ambient temperature before measurement.

2.2. Catalyst Characterization

X-ray diffraction (XRD) measurements were performed using a Philips Goniometer PW 1050/25 diffractometer equipped with a Cu$K\alpha$ X-ray source (λ: 1.5418 Å). To determine the average Au particle size and particle size distribution, transmission electron microscopy (TEM) was performed using a Philips CM30T electron microscope equipped with a LaB_6 filament as the source of electrons operated at 300 kV. The samples were mounted on a microgrid carbon polymer supported on a copper grid by placing a few droplets of a suspension of ground catalyst in ethanol on the grid, followed by drying at ambient conditions.

The Au loading was determined by atomic absorption spectroscopy (AAS) using a Perkin Elmer 3100 with an air/acetylene flame. For that purpose, the catalysts were dissolved in hot aqua regia. Subsequently, the solution was cooled and diluted with demineralized water.

2.3. Catalyst Testing

The methane oxidation measurements were performed in a fixed bed microreactor. Prior to measurement, the catalyst (0.200 g) was once again heated in 4 vol% H_2 in He up to 300°C (heating rate 10°C min^{-1}) and kept at this temperature for half an hour. Subsequently the catalyst was cooled to room temperature in a flow of He before the reactant gas was introduced. CH_4 (0.8 vol%) and O_2 (3.2 vol%) balanced in He were passed over the catalyst bed at a GHSV of ca. 1500 h^{-1}. After a stabilization time of 30 min at room temperature, two reaction cycles were recorded in the temperature range of 200 to 740°C. On-line gas analysis was performed using a Chrompack CP9001 gas chromatograph equipped with a Hayesep N column and flame ionization detector (FID).

3. RESULTS

3.1. Characterization of Au/Al_2O_3 Catalysts

The Au loading was determined by flame AAS. The results are summarized in Table 1. It is clear that the catalysts did not loose any of the Au phase during the reaction due to evaporation or complexation of Au. Striking though, is the small amount of Au initially present on catalyst C. Only about 50% of the intended Au loading was reached at pH 8. Chang *et al.* (33) also noted an incomplete deposition of Au onto Al_2O_3 at pH values between 6 and 9, but failed to give a proper explanation. To investigate the origin of this poor deposition more specifically, several other catalysts were prepared that were similar to catalyst C, but now over a pH ranging from 6 to 12. These were also characterized by AAS. The results are shown in Fig. 1. The Au loading was found to depend strongly on the final pH of the precipitation solution. At pH values higher than 8.5 a sharp decrease in Au loading was observed. A similar pH dependency was found by Li *et al.* (34) for the deposition of Pd on Al_2O_3/Al.

TABLE 1

AAS, XRD, and TEM Study of Au/Al_2O_3 Catalysts

	Au loading $(wt\%)_{AAS}$		Mean diameter $(nm)_{XRD}$		Mean diameter $(nm)_{TEM}$	
Catalyst	Fresh	Used	Fresh	Used	Fresh	Used
A	4.8	5.0	43.8	43.2	—	—
B	4.7	4.8	34.6	36.7	—	—
C[a]	2.6	2.9	3.0	6.8	3.9 ± 1.2	7.4 ± 2.7
D	5.1	5.1	2.7	11.0	3.6 ± 1.4	9.7 ± 4.0

[a] Final preparation pH 8.

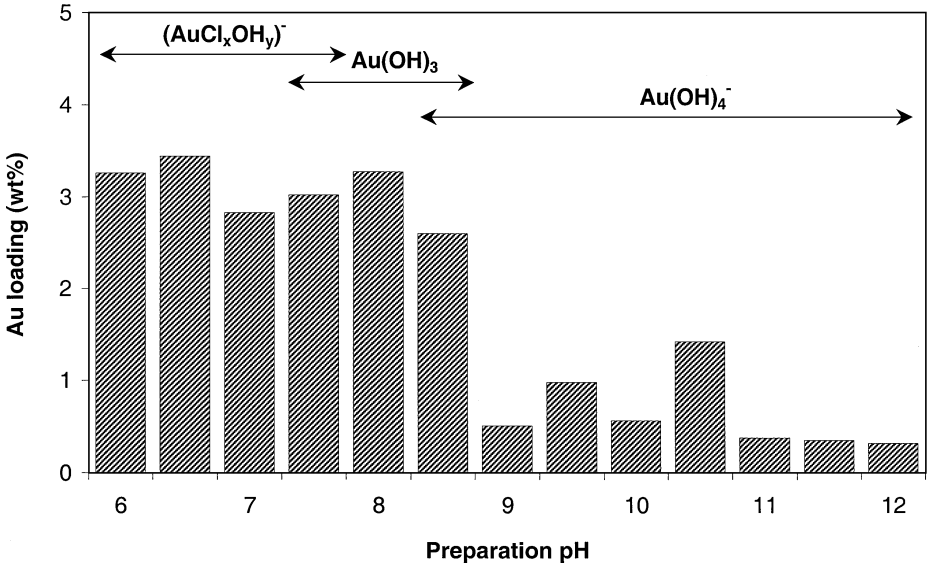

FIG. 1. Au loading on Al_2O_3 versus final pH during deposition precipitation using Na_2CO_3 as precipitating agent (catalyst C).

X-ray diffraction patterns were typically measured from $1.82 < d < 2.98$ nm. In this region the two most intense diffraction peaks of metallic gold, Au(111) at 2.355 nm and Au(200) at 2.039 nm, can be monitored. Diffraction patterns of reduced Au/Al_2O_3 were corrected for diffraction caused by the support, and are shown in Fig. 2. Both catalysts prepared via impregnation methods (catalysts A and B) show intense diffraction peaks of metallic Au, whereas the Au phase on the catalysts prepared via HDP (catalysts C and D) is hardly visible. This can be due to a lack of sufficient crystalline material present (low loading, or amorphous material). However, since the intended Au loading is sufficiently high, and Au tends to crystallize easily on MO_x, this is probably caused by severe line broadening, which is typical of (very) small particles. The line broadening of the diffraction peaks is an indication of the average particle size of crystallites. Provided that the particle sizes are between approximately 3 and 50 nm, an estimation of the average particle size can be made by using the simple Scherrer equation (35) (Table 1). The diffraction pattern of catalyst

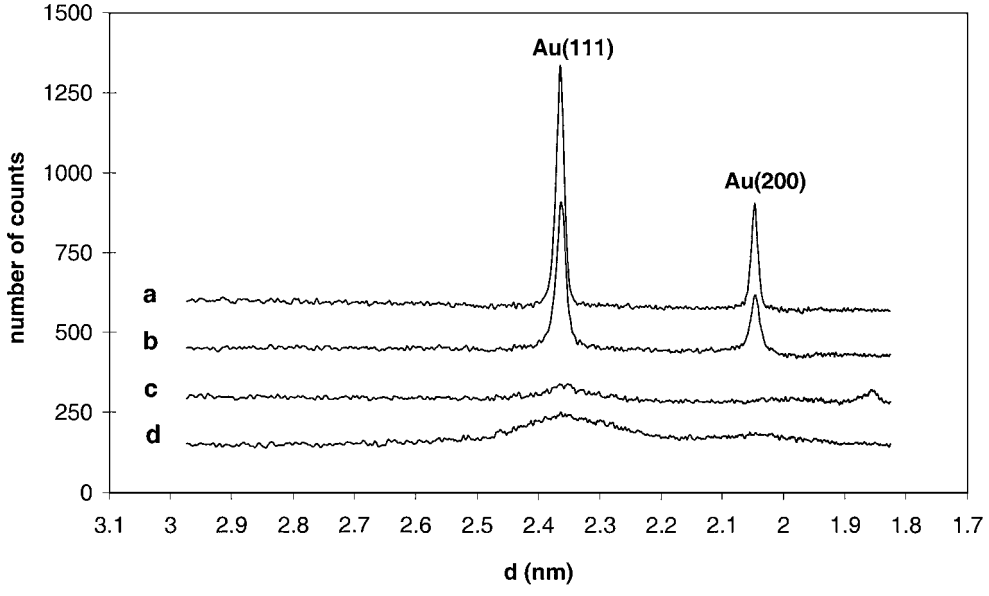

FIG. 2. X-ray diffraction patterns after reduction at 300°C in H_2 for 30 min (heating rate 5°C min^{-1}) of Au/Al_2O_3 prepared via pore volume impregnation (a), wet impregnation (b), HDP with Na_2CO_3 (c), and HDP with $NH_2(CO)NH_2$ (d).

C shows an additional feature at 1.852 nm. This feature is probably caused by an impurity originating from Na_2CO_3 and was no longer detected after CH_4 oxidation. For all catalysts, before and after reaction, metallic Au was the only phase detected. Neither Au_2O nor Au_2O_3 was found. Additionally, XPS analysis of the studied catalysts was performed, but did not result in better insights into the oxidation state of Au.

Catalysts C and D were studied in more detail using TEM. Figures 3 and 4 show TEM images and Au particle size distributions of catalyst D, respectively. Before reaction, both catalysts C and D were found to have a similar average particle size (Table 1) and particle size distribution. After reaction, the small Au particles initially present on both catalysts had disappeared. However, the particles on catalyst C were subject to sintering to a much lesser extent than on catalyst D. This is in good agreement with XRD results. When a particle is well oriented, TEM can achieve a resolution in which the separate lattice planes can be visualized (Fig. 3c). When detected, the only lattice spacing found in catalysts C and D, both before and after reaction, was about 2.32 nm. This is within the experimental error for the Au(111) reflection and does not support the presence of any oxidic Au species.

3.3. *Oxidation of Methane over Au/Al_2O_3 Catalysts*

Figure 5 shows a typical activity experiment performed on catalyst D. After the first heating stage a clear deactivation was observed. Further reaction cycles did not influence the activity significantly. This deactivation was most pronounced for the catalysts prepared via HDP with either Na_2CO_3 (catalyst C) or $NH_2(CO)NH_2$ (catalyst D) used as precipitating agent.

The data were fit to a sigmoidal distribution function of the following form;

$$\alpha = b \cdot [1 - \exp\{-(k \cdot (T - c))^d\}], \qquad [1]$$

in which α is the fraction of CH_4 consumed, T the temperature of the reactor, and b, k, c, d are constants. These constants were varied until the best fit was found. In the temperature range studied, all catalysts showed complete oxidation of CH_4, i.e., no CO was detected. The temperature of the maximum of the derivative of [1] provides a good parameter to compare different catalysts and will further be noted as $(d\alpha/dT)_{max}$. The $(d\alpha/dT)_{max}$ of the investigated catalysts for the complete oxidation of CH_4 are summarized in Table 2. Bare Al_2O_3 was found to be considerably less active than the Au-containing catalysts in the temperature range studied.

The Arrhenius plots for CH_4 oxidation over the different Au/Al_2O_3 catalysts are shown in Fig. 6. The apparent activation energies (E_a) were calculated at conversions ranging from 0.05 to 0.20 (Table 2). No significant mass transfer limitations were observed in this region. The E_a was found to

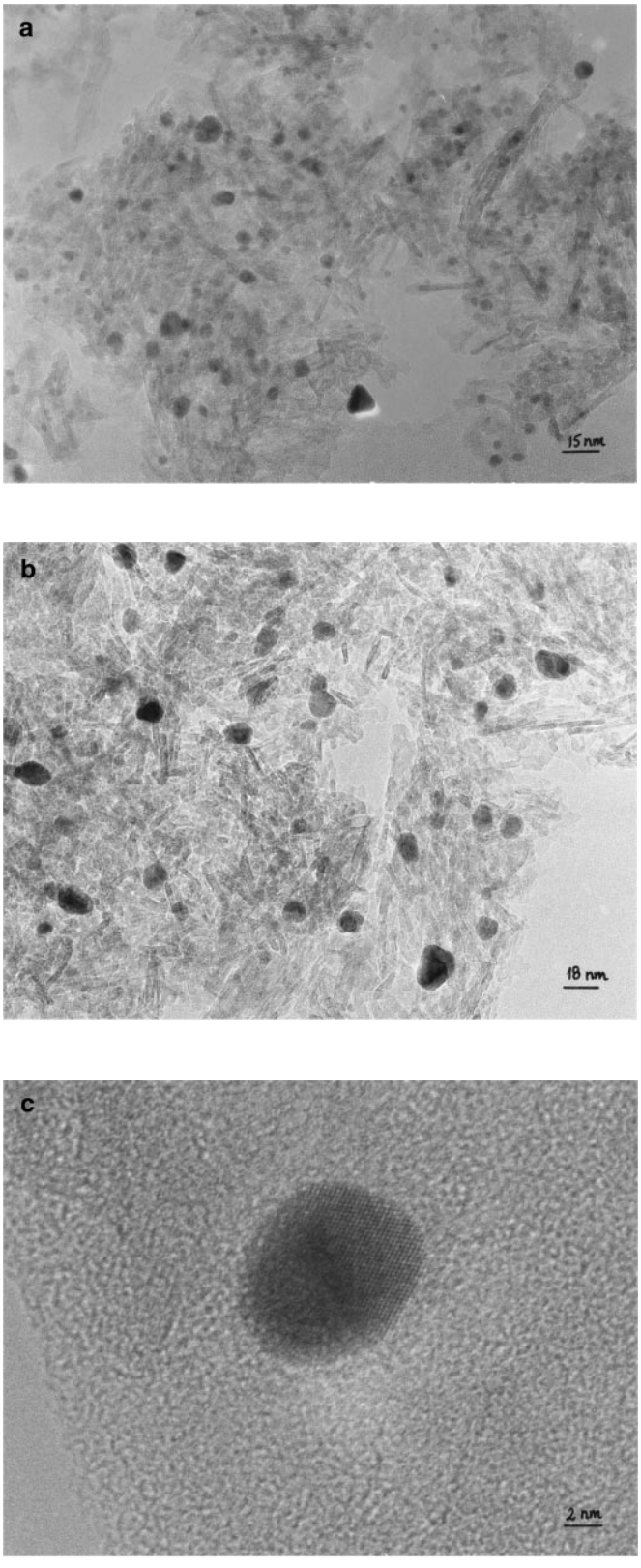

FIG. 3. TEM photographs of Au/Al_2O_3 prepared via HDP with $NH_2(CO)NH_2$ (catalyst D) before (a) and after (b) two runs of a heating and cooling cycle in the CH_4 oxidation by O_2. Lattice spacing of a Au particle of catalyst D before reaction (c).

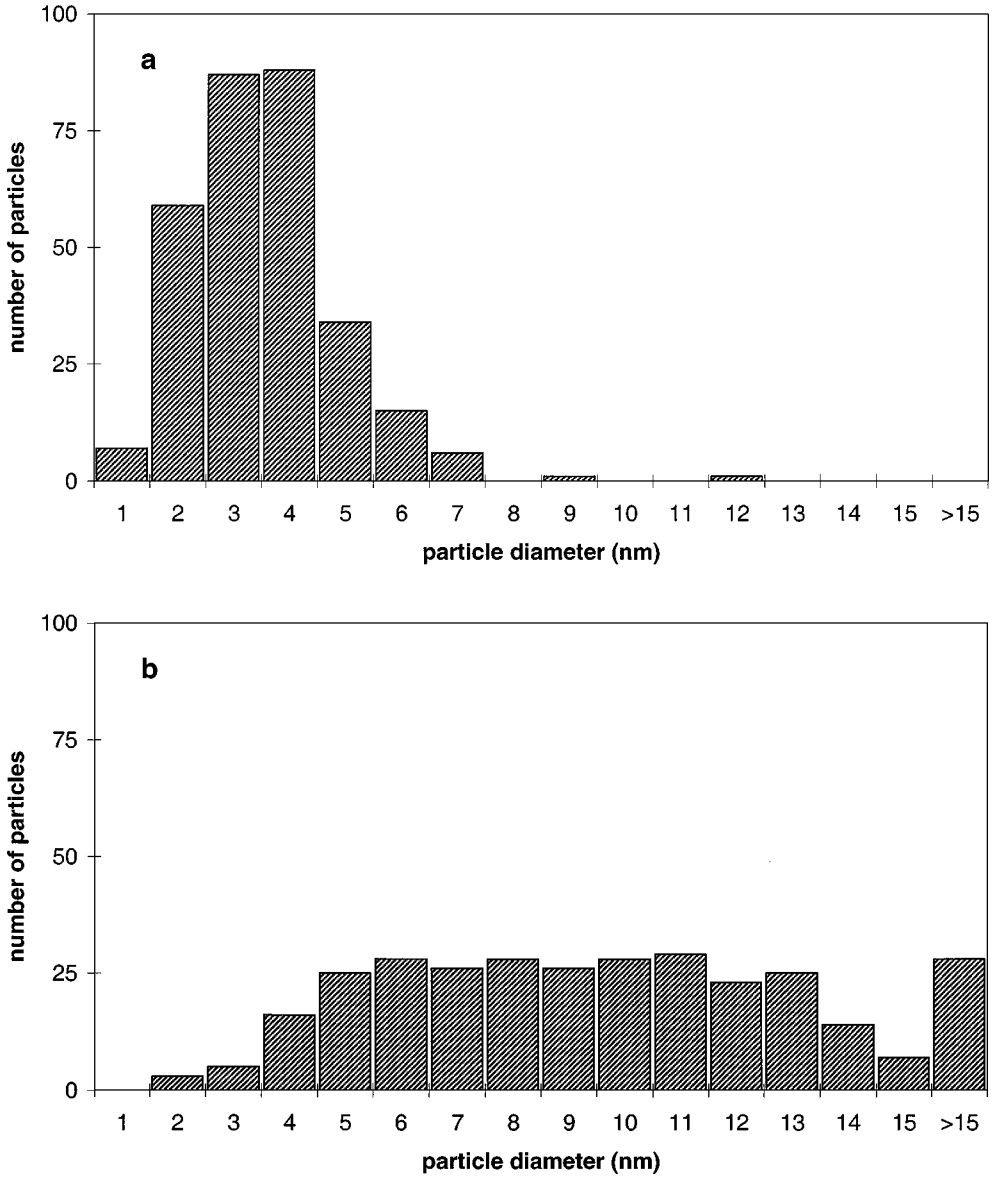

FIG. 4. Size distribution of Au particles supported on Al_2O_3 prepared via HDP with $NH_2(CO)NH_2$ (catalyst D) before (a) and after (b) two runs of a heating and cooling cycle in the CH_4 oxidation by O_2.

TABLE 2

Methane Oxidation over Au/Al_2O_3 Catalysts

Catalyst	$(d\alpha/dT)_{max}$ (°C)[a]	E_a (kJ mol^{-1})	References
Al_2O_3	—[b]	140 ± 4[a]	—
A	716	100 ± 4[a]	—
B	698	88 ± 3[a]	—
C	622	78 ± 3[a]	—
D	574	73 ± 3[a]	—
Pd/Al_2O_3	—	70–95	(32, 36–40)
Pt/Al_2O_3	—	100–125	(38, 41, 42)

[a] Second heating curve.
[b] CH_4 conversion stays below 0.50 in the temperature range studied.

increase with increasing average Au particle size, whereas the preexponential factor decreased.

It is clear that the activity of both catalysts prepared via impregnation techniques (catalysts A and B) is inferior to those prepared via HDP (catalysts C and D), which reached full conversion of CH_4 into CO_2 at about 700–750°C. The apparent activation energies of the latter are similar to those reported for Pd (32, 36–40) but significantly lower than those reported for Pt (38, 41, 42).

4. DISCUSSION

The intended Au loading on all catalysts was experimentally affirmed except for those prepared via HDP using

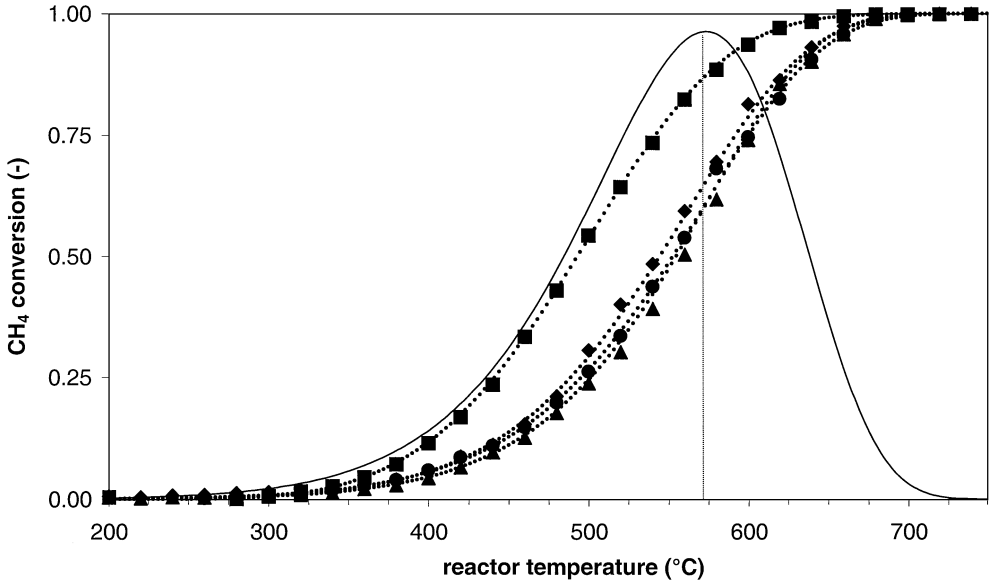

FIG. 5. CH_4 conversion versus temperature over Au/Al_2O_3 prepared via HDP with $NH_2(CO)NH_2$ as precipitating agent (catalyst D). First heating stage (■), first cooling stage (◆), second heating stage (▲), second cooling stage (●). Sigmoidal fits (···), derivative of second heating stage (—).

Na_2CO_3 as precipitating agent. The final pH of the preparation solution affected the amounts of deposited Au enormously. In acidic solutions, Al_2O_3 is partly protonated leaving an overall positively charged surface. Most of the Au precursor then is present as $AuCl_n(OH)_{4-n}^-$ and adsorption will occur via electrostatical interaction and ion-exchange reactions. At pH values around 7–8 most of the Cl^- will be displaced by OH^- leaving neutrally charged $Au(OH)_3$, which precipitates out of the solution. When in basic solution, the $Au(OH)_3$ can dissolve again as $Au(OH)_4^-$. Moreover, the surface of Al_2O_3 is deprotonated and will mostly exist as $Al\text{-}O^-$, which complicates interaction with the negatively charged precursor complex. The amount of Au adsorbed probably also depends on the speed of Na_2CO_3 addition. In solution, $Au(OH)_3$ will much more easily become coordinated by an additional OH^- than deposited on Al_2O_3. This might be the cause of lower Au loading on these samples than when using $NH_2(CO)NH_2$, which causes a

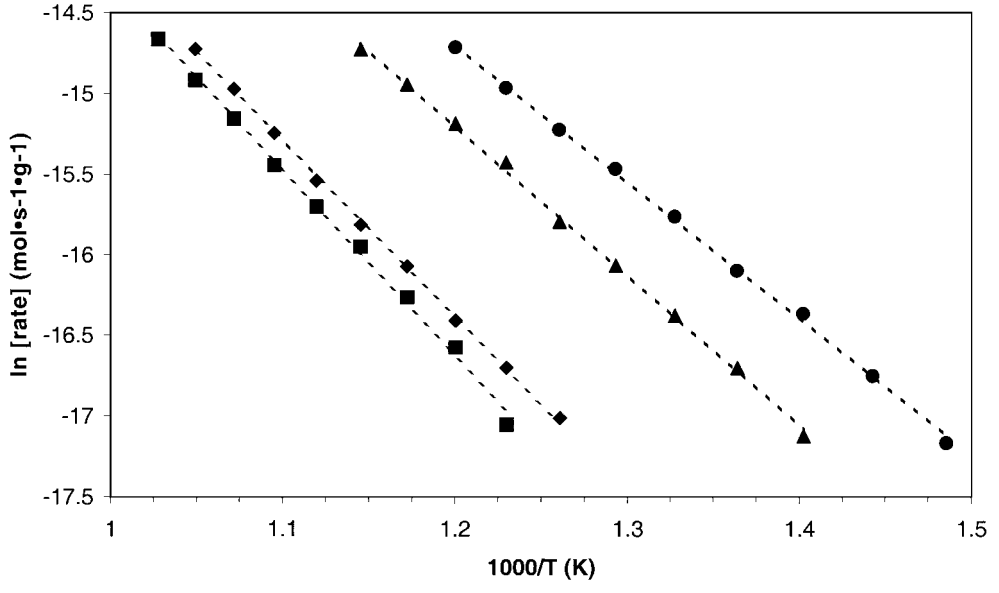

FIG. 6. Arrhenius plots for CH_4 oxidation versus the reciprocal temperature (K). Au/Al_2O_3 prepared via pore volume impregnation (■), wet impregnation (◆), HDP with Na_2CO_3 (▲), and HDP with $NH_2(CO)NH_2$ (●).

slower and more homogeneous pH of the solution at 70°C (43, 44).

It has been reported for low temperature CO oxidation that a small average particle size is beneficial for high catalytic activity at low temperature (19, 21–23). The high activity is generally attributed to the presence of a long Au/MO_x perimeter (15, 45), or special sites present only on small Au particles, such as coordinately unsaturated Au surface atoms (46), sites with an altered electronic structure (47), or ionic Au (23, 30, 33). The present results show that also for CH_4 oxidation small Au particles (3–10 nm) exhibit a much higher activity at the high temperatures (700°C) required for CH_4 oxidation.

It is known that Al_2O_3 tends to form spinel-type species with a number of transition metals and rare earth metals. Therefore Au ions incorporated in the Al_2O_3 lattice could provide for another type of active site for the oxidation of CH_4. It is, however, rather unlikely that Al^{3+} is substituted by Au^{3+}, regarding the effective ionic radius of the latter being more than 1.5 times bigger (48). Moreover, no Au spinel types have been reported up to now. However, Au containing $M_2Au_2X_6$ (M = Rb, Cs; X = Cl, Br, I) perovskites (49, 50) and M_3AuO (M = K, Cs, Rb) anti-perovskites (51, 52) do exist. In these structures the presence of an intermediate-sized alkali metal with a low ionization potential seems to be inevitable. The only other reported, non-alkali metal perovskites are iron-gold nitride $AuFe_3N$ (53), $La_2Au_{0.5}Li_{0.5}O_4$ (54), and Au-substituted superconductor $Ba_2Y(Cu_{1-x}Au_x)_3O_{7-\delta}$ ($0 < x < 0.1$) (55, 56).

Only catalysts with initially small Au particles (catalysts C and D) showed significant sintering, and a decrease in activity after the first heating curve. The fact that catalyst C is inclined to sinter to a lesser extent than catalyst D is most likely due to the lower Au loading obtained for catalyst C. The specific surface areas of the different catalysts were measured before and after reaction. All freshly prepared catalysts were found to have similar surface areas as the bare support (200 $m^2\ g^{-1}$). Also after reaction no change was detected. The observed decrease in catalyst performance after the first heating curve (Fig. 5) can thus not be explained by loss of surface area.

Although both XRD and TEM data only affirm the presence of metallic Au, it cannot be excluded a priori that very small Au clusters with ionic character may be present on the surface, and might be responsible for the observed activity. However, even the smallest Au particles detected with TEM (about 1 nm) showed only *d*-spacing characteristic of metallic Au and no indication of ionic species was obtained. Regarding the particle size distributions of catalysts C and D, and since 1 nm Au crystallites form only a minor fraction of the monitored particles (Fig. 4a), the existence of even smaller particles, which cannot be resolved by TEM under the applied conditions, is unlikely. This becomes even more improbable after reaction (Fig. 4b). So, if there were any ionic Au species on the surface, this would be only a very small fraction of the total amount of deposited Au. In addition, it is questionable that ionic Au species can survive a temperature of 740°C since gold oxide already decomposes at a temperature of 160–250°C in air (48). Therefore, our results do not support the model that ionic Au species would be responsible for the observed activity. Moreover, recently it was reported that Au/TiO_2 needed a reductive pretreatment to obtain high catalytic activity for the oxidation of CO at ambient temperature (24). This indicates that metallic Au can be the catalytically active component.

The CH_4 oxidation activity was found to depend on the average Au particle size. Whereas the presence of mainly large Au agglomerates improves the activity over Al_2O_3 only a little, small Au particles were found to improve the activity to a large extent. Furthermore, also the E_a merely seems to be correlated to the average Au particle size. Similar results were observed by Hicks *et al.* [42] for CH_4 oxidation over Pd/Al_2O_3. This particular behavior can be explained by assuming the presence of multiple active sites for the oxidation of CH_4 on Au-supported catalysts, all with different E_a. Sites involving a low E_a are predominantly present on small Au crystallites, e.g., coordinately unsaturated Au surface atoms or surface atoms at the Au/MO_x interface, whereas sites with higher E_a are relatively more abundant on larger Au particles or the support, e.g., metallic Au sites and lattice defects in MO_x. The measured E_a then is merely an average of the E_a of all the sites present on the catalyst.

5. CONCLUSIONS

The $(d\alpha/dT)_{max}$ and apparent activation energies found in this study for the total oxidation of CH_4 over different Au catalysts clearly indicate a particle size effect of Au on the activity of these catalysts. The preparation technique has a large influence on the obtained average particle size and, hence, on the activity. The best performing catalysts are obtained via homogeneous deposition precipitation. However, some deactivation has been found due to sintering of the Au particles. The oxidation activity and E_a seem to be correlated to the average Au particle size. This might imply a model in which different sites on the catalyst are active in CH_4 oxidation. The results presented in this work do not support the idea of ionic Au as active species.

ACKNOWLEDGMENTS

This work has been performed under auspices of NIOK, the Netherlands Institute for Catalysis Research, Lab Report No. UL 99-2-08. The financial support of NWO is acknowledged.

REFERENCES

1. Sakurai, H., Tsubota, S., and Haruta, M., *Appl. Catal. A* **102**, 125 (1993).
2. Sakurai, H., and Haruta, M., *Appl. Catal. A* **127**, 93 (1995).
3. Baiker, A., Kilo, M., Maciejewski, M., Menzi, S., and Wokaun, A., *in* "New Frontiers in Catalysis" (L. Guczi, F. Solymosi, and P. Tetenyi, Eds.), p. 1257. Elsevier, Amsterdam, 1992.
4. Nkosi, B., Coville, N. J., Hutchings, G. J., Adams, M. D., Friedl, J., and Wagner, F. E., *J. Catal.* **128**, 366 (1991).
5. Nkosi, B., Adams, M. D., Coville, N. J., and Hutchings, G. J., *J. Catal.* **128**, 378 (1991).
6. Ueda, A., Oshima, T., and Haruta, M., *Appl. Catal. B* **12**, 81 (1997).
7. Lee, J. Y., and Schwank, J., *J. Catal.* **102**, 207 (1986).
8. Salama, T., Ohnishi, R., Shido, T., and Ichikawa, M., *J. Catal.* **162**, 169 (1996).
9. Salama, T., Ohnishi, R., and Ichikawa, M., *J. Chem. Soc. Faraday Trans.* **92**, 301 (1996).
10. Salama, T., Ohnishi, R., and Ichikawa, M., *Chem. Commun.* 105 (1997).
11. Dekkers, M. A. P., Lippits, M. J., and Nieuwenhuys, B. E., *Catal. Today*, in press.
12. Bollinger, M. A., and Vannice, M. A., *Appl. Catal. B* **8**, 417 (1996).
13. Okumura, M., Tsubota, S., Iwamoto, M., and Haruta, M., *Chem. Lett.*, 315 (1998).
14. Liu, Z. M., and Vannice, M. A., *Catal. Lett.* **43**, 51 (1997).
15. Grunwaldt, J.-D., and Baiker, A., *J. Phys. Chem. B* **103**, 1002 (1999).
16. Grunwaldt, J.-D., Kiener, C., Wögerbauer, C., and Baiker, A., *J. Catal.* **181**, 223 (1999).
17. Cunningham, D., Tsubota, S., Kamijo, N., and Haruta, M., *Res. Chem. Intermed.* **19**, 1 (1993).
18. Lin, S., Bollinger, M., and Vannice, M., *Catal. Lett.* **17**, 245 (1993).
19. Haruta, M., Tsubota, S., Kobayashi, T., Kageyama, H., Genet, M., and Delmon, B., *J. Catal.* **144**, 175 (1993).
20. Srinivas, G., Wright, J., Bai, C., and Cook, R., *Stud. Surf. Sci. Catal.* **101**, 427 (1996).
21. Haruta, M., Yamada, N., Kobayashi, T., and Iijima, S., *J. Catal.* **115**, 301 (1989).
22. Tanielyan, S., and Augustine, R., *Appl. Catal. A* **85**, 73 (1992).
23. Boccuzzi, F., Chiorino, A., Tsubota, S., and Haruta, M., *Catal. Lett.* **29**, 225 (1994).
24. Dekkers, M. A. P., Lippits, M. J., and Nieuwenhuys, B. E., *Catal. Lett.* **56**, 195 (1998).
25. Nieuwenhuys, B. E., *in* "Elementary Reaction Steps in Heterogeneous Catalysis" (R. W. Joyner and R. A. van Santen, Eds.), p. 168. Kluwer, Dordrecht, 1993.
26. Chen, B., Bai, C., Cook, R., Wright, J., and Wang, C., *Catal. Today* **30**, 15 (1996).
27. Nakatsuji, H., Hu, Z.-M., Nakai, H., and Ikeda, K., *Surf. Sci.* **387**, 328 (1997).
28. Nijhuis, T. A., Huizinga, B. J., Makkee, M., and Moulijn, J. A., *Ind. Eng. Chem. Res.* **38**, 884 (1999).
29. Hayashi, T., Tanaka, K., and Haruta, M., *J. Catal.* **178**, 566 (1998).
30. Waters, R. D., Weimer, J. J., and Smith, J. E., *Catal. Lett.* **30**, 181 (1995).
31. Blick, K., Mitrelias, T. D., Hargreaves, J. S. J., Hutchings, G. J., Joyner, R. W., Kiely, C. J., and Wagner, F. E., *Catal. Lett.* **50**, 211 (1998).
32. Ribeiro, F. H., Chow, M., and Dalla Betta, R. A., *J. Catal.* **146**, 537 (1994).
33. Chang, C.-K., Chen, Y.-J., and Yeh, C.-T., *Appl. Catal. A* **174**, 13 (1998).
34. Li, X. H., and An, L. D., *Korean J. Chem. Eng.* **15**, 563 (1998).
35. Scherrer, P., Nachr. k. Ges. Wiss., Göttingen 98, 1918.
36. Cullis, C. F., Keene, D. E., and Trimm, D. L., *J. Chem. Soc. Faraday Trans.* **67**, 864 (1971).
37. Cullis, C. F., Keene, D. E., and Trimm, D. L., *J. Catal.* **19**, 378 (1970).
38. Yu Yao, Y.-F., *Ind. Eng. Chem. Prod. Res. Dev.* **19**, 293 (1980).
39. Baldwin, T. R., and Burch, R., *Appl. Catal.* **66**, 337 (1990).
40. Baldwin, T. R., and Burch, R., *Appl. Catal.* **66**, 359 (1990).
41. Lee, J. H., and Trimm, D. L., *Fuel Process. Technol.* **42**, 339 (1995).
42. Hicks, R. F., Qi, H., Young, M. L., and Lee, R. G., *J. Catal.* **122**, 280 (1990).
43. Geus, J. W., Dutch Patent Appl. 6,705, 259, 1967.
44. Geus, J. W., *in* "Preparation of catalysts III" (G. Poncelet, P. Grange, and P. A. Jacobs, Eds.), p. 1. Elsevier, Amsterdam, 1983.
45. Haruta, M., *Catal. Surv. Jpn.* **1**, 61 (1997).
46. Ruff, M., Frey, S., Gleich, B., and Behm, R. J., *Appl. Catal. A* **66**, S513 (1998).
47. Valden, M., Lai, X., and Goodman, D. W., *Science* **281**, 1647 (1998).
48. "Handbook of Chemistry and Physics" (R. C. Weast and M. J. Astle, Eds.) 63rd ed. CRC Press, Boca Raton, FL, 1982–1983.
49. Kojima, N., Hasegawa, M., Kitagawa, H., Kikegawa, T., and Shimomura, O., *J. Am. Chem. Soc.* **116**, 11368 (1994).
50. Kojima, N., Fukuhara, F., Kitagawa, H., Takahashi, H., and Mori, N., *Synthetic Met.* **86**, 2175 (1997).
51. Feldmann, C., and Jansen, M., *Z. Anorg. Chem.* **621**, 201 (1995).
52. Feldmann, C., and Jansen, M., *Z. Anorg. Chem.* **621**, 1907 (1995).
53. De Figueiredo, R. S., Kuhnen, C. A., and Dos Santos, A. V., *J. Magn. Magn. Mat.* **173**, 141 (1997).
54. Abbattista, F., Vallino, M., and Mazza, D., *J. Less-Common Met.* **110**, 391 (1985).
55. Hepp, A. F., Gaier, J. R., and Pouch, J. J., *J. Solid State Chem.* **74**, 433 (1988).
56. Streitz, F. H., Cieplak, M. Z., Gang Xiao, Gavrin, A., Bakhshai, A., and Chien, C. L., *Appl. Phys. Lett.* **52**, 927 (1988).